2250

FAILURE MODE CLASSIFICATION OF REINFORCED CONCRETE COLUMNS BY THE ANALYSIS OF THE STRAIN DISTRIBUTION IN THE MAIN REINFORCEMENT

Primo Allan T ALCANTARA[1] And Hiroshi IMAI[2]

SUMMARY

A new approach in the classification of the resulting failure mode, whether shear, bond splitting or flexure, for reinforced concrete columns is presented. Particular emphasis is placed on the analysis of the strain distribution in the main reinforcement based on the truss and arch model theory. The proposed alternative method is compared with results from several series of column experiments. The proposed method is shown to provide a high precision in classifying failure modes with consideration of the presence of inner rows of main bars and axial loading.

INTRODUCTION

Failure of a reinforced concrete member, such as columns, are classified into three major types: shear, bond splitting and flexural modes. Although it is common practice to rely on the observed crack patterns and the yielding of the steel reinforcement to determine the resulting failure mode, problems arose for specimens exhibiting features of more than one type of failure mode. Hence, there is difficulty in the evaluation of the ultimate strength of the columns, especially whether it be for shear or for bond splitting.

An alternative approach in the classification of failure modes for reinforced concrete columns [Alcantara 1999] is presented. Aside from failure mode classification by the use of crack patterns, bar strains and ultimate strengths, an analysis of the strain distribution in the main reinforcement is considered. Using the proposed method gives a different perspective wherein focus is given from within the interior of the column showing the actual behavior of the main reinforcement under loading. Test results on reinforced concrete columns showing the strain distribution in the main reinforcement were used and compared, both qualitatively and quantitatively, with the theoretical strain distribution using the truss and arch model.

TRUSS AND ARCH MODEL THEORY

Predicting resulting failure modes is very essential in the design of columns to assure safety and adequate resistance to earthquake forces. Although there are existing equation regarding the shear, bond splitting and flexural capacities of columns, results showed some inconsistencies with regard to the theoretical and experimental values as well as the observed crack patterns and reinforcing bar strains. The truss and arch mechanisms were used in the calculations involving the shear and bond splitting capacities of columns while the ultimate strength concept was applied for the flexural capacities. Moreover, a comparison of the theoretical strain distribution to the experimental strain distribution in the main reinforcement based on each of the failure modes was done. The truss and arch model was also used in the calculations of the theoretical strains for the shear and bond splitting types while the equilibrium and strain compatibility assumptions were used for the flexural type. Finally, failure mode classification was performed using the data gathered.

Column Capacity

Failure of a column depends on its overall strength. Since the column could fail in either shear, bond splitting or flexure, the lateral force capacities according to the various failure modes were determined. The shear capacity

[1] *Graduate Student, Institute of Engineering Mechanics, University of Tsukuba, Japan, primoallan@usa.net*

[2] *Associate Professor, Institute of Engineering Mechanics, University of Tsukuba, Japan, imai@kz.tsukuba.ac.jp*

of columns was calculated by the strength equation given in the design code of the Architectural Institute of Japan [AIJ 1994] which is as shown in Eq. (1).

$$Q_{su} = Q_{sut} + Q_{sua} = bj_t p_w \sigma_{wy} \cot\phi + \tan\theta(1-\beta)bD\nu\sigma_B/2 \tag{1}$$

The bond splitting capacity of columns is mainly dependent on the bond strength of the main reinforcement. Among the proposed equations given for the bond strength of bars are those given by Fujii-Morita [Fujii 1983] and Kaku [Kaku 1994]. In the derivation of the bond splitting capacity, the truss and arch model was also made as the basis of the shear resisting mechanism. The calculated bond strength using the proposed equations was used as the controlling parameter in the derivation of the bond splitting capacity. Accordingly, the bond splitting capacity is given by Eq. (2).

$$Q_{bu} = Q_{but} + Q_{bua} = \tau_{bu}(\Sigma\psi_h)j_t + \tan\theta(1-\beta)bD\nu\sigma_B/2 \tag{2}$$

The calculation of the flexural capacity was based on the ultimate strength concept wherein the shape of the concrete compression zone is represented by the stress-strain curve based on the e-function model [Muto 1964] and the stress-strain relationship for the main reinforcement is based on a bilinear elastic-perfectly plastic model. Considering the stress-strain conditions along the column cross section, an iterative procedure was done wherein at increasing values of the strain at the extreme compression fiber, locations of the neutral axis were determined and the corresponding values of the lateral load can be calculated by moment equilibrium. The flexural capacity, Q_{mu}, of the column corresponds to the maximum calculated value obtained from the above procedure.

Effect of Axial Loading

In the aforementioned discussion of the column capacity based on the truss and arch model, the loading condition on a regular beam, where axial loading is not applied, is considered. However, for columns, the level of axial loading is relatively high and has a considerable effect on its overall behavior. Figure 1 (a) shows a schematic diagram of the behavior of the column having an axial load, N, when subjected to lateral seismic forces. It is shown that a concrete arch will be formed along the diagonal of the column [Nigel Priestley 1994] that would partly resist the axial load applied and the remaining of which would be carried by the main reinforcement. Moreover, from equilibrium, it was derived that the lateral force due to the applied axial load, Q_{axial}, is resisted solely by the concrete arch and is given by Eq. (3).

$$Q_{axial} = \sigma_{axial} bx' \cos\theta' \sin\theta' \tag{3}$$

Such analogy is very similar to the diagram representing the column behavior due to the arch mechanism as shown in Fig. 1 (b) except for the presence of axial loading. For this case, the lateral force, Q_{arch}, is also resisted solely by the concrete arch as shown in Eq. (4).

$$Q_{arch} = \sigma_{arch} bx \cos\theta \sin\theta \tag{4}$$

In order to maximize the lateral force contribution due to the arch mechanism and the axial load, both diagrams are combined as shown in Fig. 1 (c) wherein the stress in the concrete arch is given by $\sigma_{arch}+\sigma_{axial}$ and the resulting lateral force is $Q_{arch}+Q_{axial}$. From the figure, the depth and angle of the concrete arch for both the axial and arch actions are assumed to be identical. By a similar procedure as in the arch mechanism, the lateral force due to both actions is shown by Eq. (5).

$$Q_{arch}+Q_{axial} = (\sigma_{arch}+\sigma_{axial})bD\tan\theta/2 \tag{5}$$

However, the stress in the concrete arch can be equated to the remaining concrete capacity after considering the stress carried by the truss mechanism ($\sigma_{arch}+\sigma_{axial} = \nu\sigma_B-\sigma_{truss}$). Therefore,

$$Q_{arch}+Q_{axial} = (\nu\sigma_B-\sigma_{truss})bD\tan\theta/2 \tag{6}$$

Equation (6) shows that the total lateral force due to the arch mechanism and the axial load is equivalent to the lateral force contribution due to pure arch action given in Eqs. (1) and (2) for shear and bond splitting types, respectively. It is implied that even though the axial load provides an additional contribution to the lateral force capacity, it actually causes a corresponding decrease in the pure arch action contribution. Thus, it is concluded that the presence of axial loading has no apparent effect on the previously calculated lateral force contribution due to the arch mechanism, but it has a strong influence on the straining of the main bars.

Strain Distribution in the Main Reinforcement

The application of the truss and arch model in the determination of the strain distribution in the main reinforcement is considered. For this section, only the distribution for the shear and bond splitting failure modes are dealt with. In this two cases, the level of straining in the main bars remains on the elastic range that, even though the bars are stressed under repeated cyclic loading, their behavior seems to be similar to that subjected to monotonic loading.

In the truss mechanism, the value of the strain is determined using the calculated force on the main bar based on the equilibrium of the infinitesimal stringer elements. Since the column is loaded under double bending, it is considered as point symmetric at the center of the column. Hence, from the free body diagram shown in Fig. 2, since there is no vertical load for the truss mechanism ($F_1+F_2=0$) and that the stress condition at both points in the main reinforcement lying on a plane inclined as an angle ϕ passing through the center of the column is the same ($F_1=F_2$), it can be shown that the strain is zero ($F_1=F_2=0$) at those same points in the main reinforcement. Since the force on the main bar is associated with stresses due to bond, it is directly dependent on the distance from the point of zero strain. Therefore, the resulting bond forces on the main bars for both the shear and bond splitting failure modes are represented by Eqs. (7).

$$bond\ force = p_w\sigma_{wy}b\cot\phi\, l_x\ (shear\ type)\ or\ \tau_{bu}\Sigma\psi_h l_x\ (bond\ splitting\ type) \qquad (7)$$

By converting the force to strain, the strain distribution due to the truss action in terms of the calculated capacity, Q_{truss}, is given by Eq. (8).

$$\varepsilon_{truss} = Q_{truss}l_x/[j_t(a_g/2)E] \quad where\ Q_{truss} = Q_{sut}\ (shear\ type)\ or\ Q_{but}\ (bond\ splitting\ type) \qquad (8)$$

A diagram showing the strain distribution due to the truss mechanism is provided in Fig. 3.

Next, the effect of axial loading will be incorporated into the derivation of the strain distribution in the main reinforcement due to the arch mechanism. From Fig. 4 and by simple equilibrium of forces, the axial load is resisted by both the concrete arch and the main reinforcement. Using the remaining compressive stress of the concrete for the arch mechanism with axial action, $\sigma_{arch+axial}$, the compressive force in the concrete arch is given by Eq. (9).

$$compressive\ force = \sigma_{arch+axial}bD/2\cos\theta \qquad (9)$$

By equilibrium, the resultant of the forces on all of the main bars is given by Eq. (10).

$$bar\ force = \sigma_{arch+axial}bD/2 - N \qquad (10)$$

Therefore, the strain due to the arch action with proper consideration of axial loading in terms of the calculated capacity, $Q_{arch+axial}$, is given by Eq. (11).

$$\varepsilon_{arch+axial} = (Q_{arch+axial}/\tan\theta - N)/a_gE \quad where\ Q_{arch+axial} = Q_{sua}\ (shear\ type)\ or\ Q_{bua}\ (bond\ splitting\ type) \qquad (11)$$

A diagram showing the strain distributiondue to the arch mechanism and the effect of axial loading is provided in Fig. 4.

To summarize, the strain distribution on the extreme main bars is determined by Eq. (12).

$$\varepsilon = \varepsilon_{truss} + \varepsilon_{arch+axial} \qquad (12)$$

EXPERIMENT DETAILS

Specimen

In this analysis, a total of 44 column specimens were tested consisting of 31 precast concrete and 13 monolithic types. The precast concrete specimens were constructed using the main bar post-insertion system [Imai 1993]. It is described as a process wherein at the factory, the precast concrete members are prefabricated without the presence of the main bars, and later at the construction site, the main bars are inserted and abutted at the middle portion of each member where the stresses due to seismic forces are small. This type of joint features the use of spiral steel sheaths which are hollow tubes positioned in place of the main bars in precast concrete members wherein such bars are to be later inserted during assembly. For this connection system, lapping bars are positioned alongside main bar abutments to allow for adequate force transfer.

Each of the column specimens was set under the loading apparatus composed of a number of actuators and jacks attached to suitably designed loading steel frame. These specimens were subjected to varying lateral forces that were applied in a cyclic manner producing anti-symmetric bending moment distribution while being acted upon by a constant axial load. Also, strain gauges were strategically positioned all over the specimen to measure the actual strains in the main, lapping and lateral reinforcing bars.

Crack Patterns and Bar Strains

In the determination of the resulting failure mode in an actual scaled experimentation, the most basic method would be to rely on the cracks appearing during the progress of the experiment. The location and orientation of the cracks as well as the crushing of the concrete is of great aid in the task of classifying the type of the resulting failure mode. The crack patterns shown in Photo. 1 are presented in the order of the conduction of the experiment and for each series, two specimens representing both the monolithic and precast concrete types are given for comparison. Photos. 1 (a) to (d) depict the typical shear failure [S] crack patterns wherein there are a lot of shear cracks produced together with the widening of the cracks at failure. However, bond splitting cracks were observed for the latter two specimens wherein bond splitting failure also commenced after failure in shear. Photos. 1 (e) and (f) represent the flexural failure [F] type of cracks. The cracks were concentrated at the end portions and crushing of the concrete eventually occurred as typical of flexural failure. Photos. 1 (g) and (h), on the other hand, are of the bond splitting failure [Bo] type. It can be seen that the bond splitting cracks along the extreme main bar are very much prominent. Considering the comparison between the monolithically cast specimens to that of the precast concrete type, it is evident from the similarity of the pictures that the cracking behavior of the columns is independent of the casting method applied.

Another aspect which could assist in the determination of the resulting failure mode is the actual strain on the reinforcing bars during maximum or peak loading. First, considering the experimental strain on the lateral reinforcement, it is typical in shear failure that there is yielding of the lateral reinforcement. From Fig. 5 (a), it can be observed that for the yielding type, there is a good correspondence with the crack patterns of the shear failure type. For the two plots on Fig. 5 (b), it can be seen that there is no yielding of the lateral reinforcement, and hence, those specimens are not failing in shear. Next, considering the strain in the main bars, failure by flexure is easily identified by the yielding at the end portions. Therefore, by plotting the strain distribution of the main bars of the specimens in Fig. 5 (b), further classification can be done. From Fig. 6 (a), it can be observed that there is yielding of the main bars which suggests a flexural type of failure. This further supports the observed flexural crack patterns during the experiment. Moreover, since there is no yielding of the main bars for the remaining specimens as shown in Fig. 6 (b), they can then be classified as of the bond splitting type.

ANALYSIS ON THE MAIN BAR STRAIN DISTRIBUTION

Visual Classification

Aside from the observed crack patterns and actual bar strains, failure mode classification can also be done through another approach. This is done by an analysis of the state of stress along the main reinforcement. Concepts behind the truss and arch model theory are utilized and comparisons between the experimental and theoretical strain distribution based on the various failure modes are conducted. The theoretical lines according to both the shear and bond splitting types were derived using the truss and arch model with consideration of the effect of axial loading with the assumption that the main bars are in the elastic range. Also, for the bond splitting capacity of the precast concrete columns, the diameter of the sheath is used as the working value for the diameter of the main bars. On the other hand, the theoretical distribution according to the flexural failure type is based on simple equilibrium and strain compatibility assumptions on the column cross section to include straining beyond the elastic range. Representative plots according to the resulting failure modes are shown in Fig. 7.

A generally good correspondence is observed with regard to the predicted and actual resulting failure mode based on the actual plots of the main bar strain distributions especially for Figs. 7 (a) to (e) and (g). However, for C51P and C64P in Figs. 7 (f) and (h), there is a little inaccuracy with the observed results. As for specimen C51P, although the experimental main bar strain distribution is closer to the predicted failure line, there is great offset observed. The figure shows that the main bar can be stresses a little further before failure. However, failure occurred at a lower strain level which proves an overestimation on the calculated bond splitting capacity. It is inferred that the calculated value using the given bond splitting capacity equation is generally overestimated for specimens having a combination of the use of high strength lateral reinforcement and a low lateral reinforcement ratio. Moreover, for specimen C64P, instead of an overestimation, an underestimation on both the calculated shear and bond splitting capacities were observed. This general behavior is typical of high strength concrete specimens wherein there is a low estimate of the calculated strengths especially for the shear failure mode. Therefore, additional studies are necessary with regard to these aspects.

Error Analysis

Aside from the visual determination of classifying failure modes, a quantitative approach is also possible. A more systematic procedure is presented wherein error estimates between the experimental and theoretical plots are determined and the one showing the least error gives the resulting failure mode. This is more reliable in cases where there is closeness between the theoretical failure lines especially for the shear and bond splitting types. The statistical criteria used is termed the “sum of squares of the errors” or *SSE*. In this procedure, the error is determined by the difference between the experimental strain at a point and the theoretical strain on the failure line at that same point in the main reinforcement. This is done for all points where the actual strains were measured experimentally. These values are then squared to eliminate negative errors. Finally, these values are added to give the *SSE*. Furthermore, this value can be normalized to an expression showing a percentage error between the experimental and theoretical values by taking the square root of the *SSE* over the sum of the squares of the experimental strains. The normalized values of the errors, e, for all the theoretical failure lines are determined and compared, wherein the least value would show the resulting failure mode. Table 1 gives the calculations made for the specimens considered. For the bond splitting type, only the error estimates for the bond splitting failure line using the Kaku equation are shown, since when considering the specimens featuring a clear bond splitting failure from experimentally observed crack patterns and bar strains, much lesser values of the error are given by the Kaku equation, which shows better precision than the Fujii-Morita equation.

From Table 1, by considering the least among the error estimates from the different failure modes, a general agreement between the observed or actual failure mode and the theoretical failure mode is observed. Of the 44 specimens considered, good correspondence between the actual and theoretical failure modes is observed for the 43 specimens. This shows a high level of precision of the proposed alternative approach in classifying failure modes. An error estimate of around 0.5 gives a very good correspondence with the actual failure mode. On the contrary, greater error estimates show an actual main bar strain distribution which is rather distant from the calculated failure line. This implies either an underestimation or overestimation on the theoretical ultimate strength of the column as shown by specimens C51P, C54P and C54M. Hence, such observations made on the error analysis acts as an aid in the improvement of the column design equations especially on the bond splitting aspect. As for the NG remark on specimen C64P, the main reason lies in the underestimation of the calculated shear and bond splitting capacities, thereby giving a wrong classification on the resulting failure mode.

CONCLUSIONS

This study is focused on the determination of the resulting failure mode based on the truss and arch model theory. Using the experimental strains in the main reinforcement and with proper consideration of the presence of inner main bars and axial loading, it can be concluded that the classification of the resulting failure mode is generally accurate for both the qualitative and quantitative aspects. In the case of shear and flexural failure, results show that the use of the main bar strain distribution is fairly good. On the other hand, for the bond splitting type, an improvement in the calculation of the reinforced concrete column capacity with proper consideration of the inner rows of main reinforcement is deemed necessary.

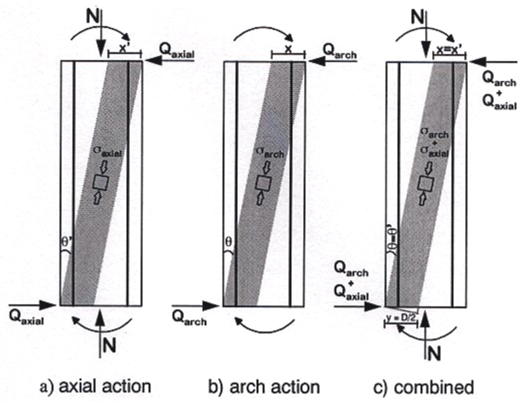

Fig. 1 Effect of Axial Loading

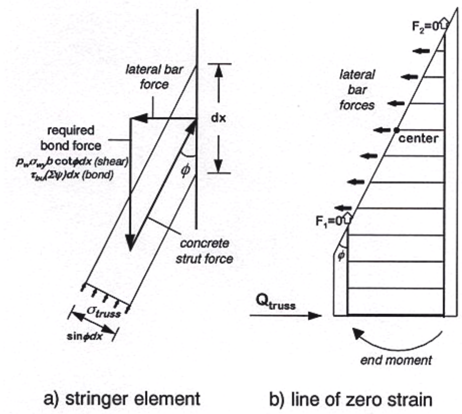

Fig. 2 Equilibrium Conditions

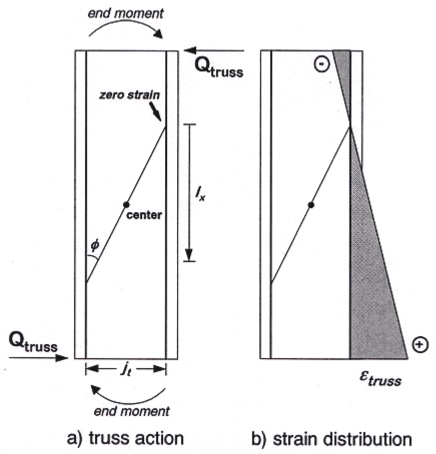

Fig. 3 Truss Mechanism

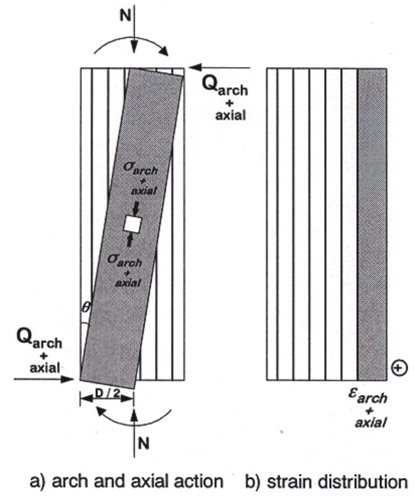

Fig. 4 Arch Mechanism and Axial Loading

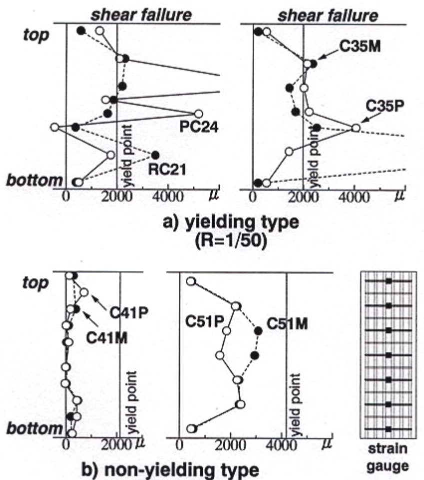

Fig. 5 Strain Distributions in the Lateral Reinforcement at Peak Load

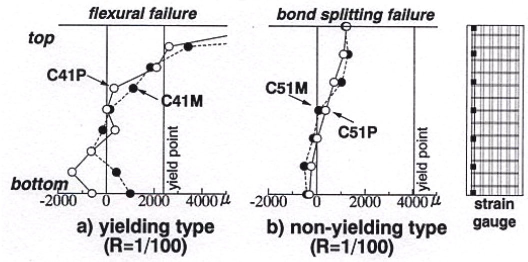

Fig. 6 Strain Distribution in the Main Reinforcement at Peak Load

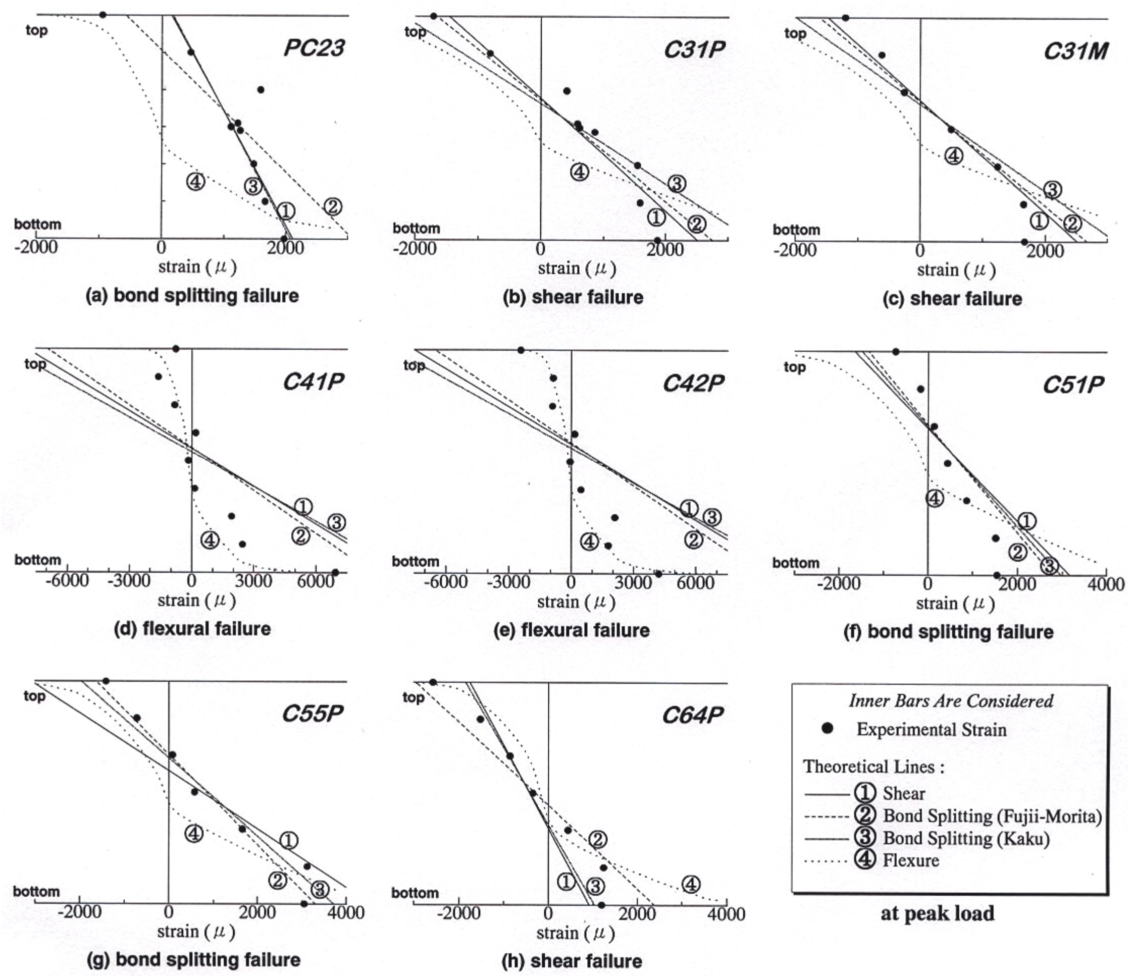

Fig. 7 Main Bar Strain Distribution

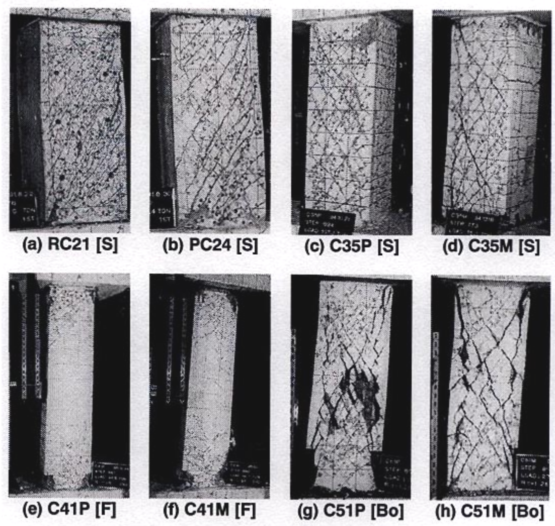

Photo. 1 Typical Crack Patterns

Table 1 Error Analysis

Specimen	Error Estimates (e)			Theoretical Failure Mode	Actual Failure Mode	Remarks
	Shear	Bond Splitting	Flexure			
RC21	**0.30**	0.39	1.55	S	S	OK
PC22	**0.24**	0.29	1.28	S	S	OK
PC23	**0.37**	**0.37**	1.93	S/Bo	Bo	OK
PC24	**0.41**	0.56	1.76	S	S	OK
PC25	0.49	0.47	**0.27**	F	F	OK
PC26	**0.59**	**0.59**	2.42	S/Bo	Bo	OK
PC27	**0.12**	0.21	0.80	S	S	OK
PC28	0.49	0.47	**0.20**	F	F	OK
C31P	**0.28**	0.56	1.45	S	S	OK
C32P	**0.29**	0.48	1.16	S	S	OK
C33P	**0.23**	0.33	0.83	S	S	OK
C34P	**0.23**	0.34	0.62	S	S	OK
C35P	**0.24**	0.29	0.38	S	S	OK
C31M	**0.31**	0.62	1.77	S	S	OK
C33M	**0.43**	0.53	1.24	S	S	OK
C35M	**0.36**	0.52	0.84	S	S	OK
C41P	2.42	2.68	**0.51**	F	F	OK
C42P	3.10	3.39	**0.55**	F	F	OK
C43P	2.02	2.18	**0.52**	F	F	OK
C44P	1.38	1.47	**0.55**	F	F	OK
C45P	2.01	2.10	**0.63**	F	F	OK
C41M	2.42	2.44	**0.48**	F	F	OK
C43M	3.06	2.97	**0.69**	F	F	OK
C45M	3.83	3.75	**1.97**	F	F	OK
C51P	0.92	**0.79**	2.91	Bo	Bo	OK
C52P	0.35	**0.11**	0.98	Bo	Bo	OK
C53P	0.68	0.67	**0.45**	F	F	OK
C54P	1.17	**1.03**	3.50	Bo	Bo	OK
C55P	0.39	**0.21**	1.14	Bo	Bo	OK
C56P	0.64	0.63	**0.44**	F	F	OK
C51M	0.61	**0.47**	2.10	Bo	Bo	OK
C53M	0.57	0.55	**0.33**	F	F	OK
C54M	0.95	**0.79**	3.10	Bo	Bo	OK
C56M	0.51	0.52	**0.50**	F	F	OK
C61M	0.37	**0.32**	1.24	Bo	Bo	OK
C61P	**0.16**	0.29	1.69	S	S	OK
C62P	**0.15**	0.44	0.66	S	S / Bo	OK
C63P	**0.17**	0.40	0.43	S	S / Bo	OK
C64P	0.35	**0.25**	1.66	Bo	S	NG
C65P	0.28	**0.23**	2.08	Bo	S / Bo	OK
C66P	**0.26**	0.46	1.05	S	S	OK
C67P	**0.15**	0.36	1.09	S	S / Bo	OK
C68P	**0.29**	0.53	0.63	S	S	OK
C68M	**0.28**	0.59	0.52	S	S / Bo	OK

S: shear Bo: Bond Splitting F: Flexure /: coincident occurrence

REFERENCES

Alcantara, P.A. and H Imai (1999). "Failure Mode Classification of RC Columns by the Analysis of the Main Bar Strain Distibution Based on the Truss and Arch Model", *Concrete Research and Technology*, 10.2, 13-28.

Architectural Institute of Japan (1994). *AIJ Structural Design Guidelines for Reinforced Concrete Buildings.*

Fujii, S. and S. Morita (1983). "Splitting Bond Capacities of Deformed Bars, Part 2 A proposed ultimate strength equation for splitting bond failure", *Transactions of the AIJ*, 324, 45-53.

Imai, H. (1993). "Precast Methods for Frame Type Buildings", *Proceedings of the Fourth International Conference on Structural Failure, Durability and Retrofitting*, 4, 396-403.

Kaku, T. et al (1994). "Influence of Yield Stress of Transverse Reinforcement on the Bond Strength of Reinforced Concrete Members", *Proceedings of the JCI*, 16.2, 247-252.

Muto, K. (1964). *Plastic Design of Reinforced Concrete Structures, Seismic Design Series 2*.

Nigel Priestley, M.J. et al (1994). "Seismic Shear Strength of Reinforced Concrete Columns", *Journal of Structural Engineering of the ASCE*, 120.8, 2310-2329.